Study on Subsonic Two-dimensional Diffuser Flows

Karanja Kibicho[1], Toyohiko Suzuki[2] and Ryoji Waka[3]

[1]Department of Mechanical Engineering, Jomo Kenyatta University of Agriculture and Technology, P.O. Box 62000, Nairobi. KENYA; [2]Department of Mechanical Engineering, Tottori University, 4-101, Minami, Koyama-Cho, Tottori-Shi 680-8552, JAPAN; [3]Faculty of Education, Tottori University, 4-101, Minami, Koyama-Cho, Tottori-Shi 680-8552, JAPAN.

ABSTRACT

A diffuser is a key element of many fluid machines and systems. Due to the large adverse pressure gradients at the diffuser entry, the diffuser flows become stalled and get attached to one wall for included angles above 7-9^0. This is accompanied by loss in static pressure recovery. This work seeks to clarify through flow visualization methods and static pressure measurements, the flow structure within the diffuser. The study was carried out for a 50^0 total included angle diffuser. Static pressure measurements along the two diverging walls were carried out. Flow visualization was conducted by use of both oil flow and wool tuft methods. The experiments were carried out for four Reynolds number of 7.2 x 10^4, 1.62 x 10^5, 2.45 x 10^5, 2.90 x 10^5. The results reveal the existence of four flow zones in the stalled diffuser flows and that there is no effect on these zones due to the change in Reynolds number.

KEY WORDS: Subsonic, two-dimensional diffuser, flow stall.

1.0 INTRODUCTION

Two-dimensional diffuser flows are flows within a diffusing passage with two parallel walls and the other walls either diverging symmetrically or unsymmetrically. This type of flow provides the most common separated flows with stalling occurring from a total included angle of 7-9^0 regardless of the Reynolds number. Practically, the flow is three-dimensional and the term two-dimensional refers more to the diffuser geometry than the flow field. Diffusers are used in practice when there is need to raise the static pressure, decelerate flow and/or change the configuration of the cross-sectional area. Some examples of practical application areas of diffusers in engineering devices are

in centrifugal compressors, pumps, gas turbines inlets, carburetors, noise suppressors, aircraft jet engines inlets, pipe systems and so on.

The principal reason why the designer can not accurately predict the diffuser performance is the fact that diffusing passages are often of small aspect ratio, three-dimensional in shape and contain boundary layer fluid over a significant part of the cross-sectional area. Therefore analytical manipulation of flows in these arbitrary passages are tedious and difficult and thus, the designer must of necessity revert to semi-empirical understanding of the flow element.

Experiments for diffuser flows are important therefore for providing the designer with design charts and data, understanding the flow dynamics and providing validation data for computational schemes.

Interest in the stalling phenomena within the diffuser flows was reported as early as 1924 (Norbury 1959). The single angle of attack to resolve the highly separated flows then was the use of the momentum integral equation in the boundary layer employing the criterion that wall shear would vanish (Schlichting 1955) at the point of stall. This theory could not account for the wide region of the separated flows and the complete stalling on one or both diverging walls.

The performance of the diffuser is affected by many factors. Chief among them are, inlet and outlet boundary layer blockage, the diffuser geometry in terms of aspect ratio and length to width ratio, wall contouring, inlet level of turbulence and the flow Reynolds number.

The inlet boundary layer thickening leads to an increase in static pressure recovery instead of the expected fall which seems to contradict the potential flow theory (Norbury 1959, Waitman *et al.* 1961, Reneau *et al.* 1967). The increase of inlet turbulence favors delay of separation and therefore increases the diffuser performance

Increase of aspect ratio is usually followed by a decrease in the blockage factor and therefore the pressure recovery increased. The increase in pressure recovery however only happens up to geometry of peak recovery for unstalled diffusers. This observation contradicts the common belief that aspect ratio does not influence the diffuser performance (Johnston and Powers 1969).

Kline (1959) in an attempt to point out disparities between results and available theory for flow in diffusing passages compared known correlations and data for stalled flows. He described stall as a point along the wall in which $\frac{\partial u}{\partial y} = 0$. With this definition boundary layer equations could be used to predict a point at which first stall occurs. The numerical prediction disagreed with measured data because the presence of stall practically altered the pressure distribution, a fact which was not accounted for in the numerical methods. He noticed the asymmetry of the flow, with the flow being attached to any wall arbitrarily. The onset of large transitory stall was unaffected by turbulence levels at inlet apart from at very low values of length to width ratios and high values of total included angle and was weakly dependent on Reynolds number and aspect ratio. The performance of high angle diffusers was improved to almost twice by use of short vanes at the inlet as long as they were short enough and the passage they formed had a total included angle of less than 8^0. Introduction of thin plates into the flow gave no appreciable change to the pressure distribution but completely changed the boundary layer structure. This contradicted the known belief then that flow pattern was determined by pressure distribution and the history of the boundary layer alone. The optimum length to width ratio was found to be 25-30 and the area ratio seemed to have no significant effect on the pressure recovery.

The ideal diffuser flow can be estimated to be a source flow with the origin at the point of intersection of the diverging walls if they are extended upstream of the throat. If the origin is translated along the centerline downstream, the effect would be equivalent to having a flow with streamlines diverging more than the walls and therefore separation would be suppressed. This principle has been used to design for vanes at the inlet of very wide-angle (Feil 1964).

Wall contouring has no effect on the overall pressure recovery even though the local pressure recovery and the location of the first stall are severely affected (Carlson *et al.*, 1967).

The most important requirement to obtain good results for steady fully separated flows is to account for exit blockage in the free shear layer and the separated region. For flows without reattachment, a free streamline solution provides an adequate modelling for

the downstream flow (Woolley and Kline, 1978). Senoo and Nishi (1977) numerically investigated the relationship between blockage factor and boundary layer shape factor at the onset of separation in a bid to predict whether or not separation occurs in a diffuser. Their work utilized the flow stability criterion to establish separation point. They concluded that local value of blockage factor determined the stability of the flow. The higher it was, the more stable was the flow. They predicted the separation point as well as the overall performance for low divergence angle diffusers.

Using the large eddy simulation (LES) numerical approach, Katelnbach *et al.* (1999), predicted separation on both walls immediately after the throat and a small detached flow at the throat which was followed by large separation of mean flow resulting into strong pressure fluctuations and turbulence production. Wide range of time scales were observed and they called for very lengthy integration times. The near wall turbulence was predicted to be out of geometry and not by pressure gradient. The rear part of the expansion showed a separation zone that was thought as a low frequency unsteady process involving large scales of motion that filled the entire cross-section.

The main objectives of the proposed study are to provide performance data for undisturbed inlet flow, the performance data with separation fixed at the diffuser inlet for total included angle of 50^0 and to provide a flow visualization study for the entire flow field. The tests were carried out at several Reynolds number in the order of 1×10^5.

2.0 EXPERIMENTAL SET-UP AND METHODOLOGY

Shown in Figure 1 is the configuration and the dimensions of the flow facility. Flow was provided through a 1m long, 200mm by 100mm rectangular inlet duct, which was connected to a square-rectangular nozzle. The existing wind tunnel had a 400mm square outlet.

The flow velocity was controlled through a frequency inverter. The static pressure holes were placed at 10mm apart near the diffuser inlet, 20mm apart further away and at 50mm apart near the exit. Velocity distribution profiles were measured both vertically and horizontally by use of a pitot-static tube. This was done for both nozzle exit and the inlet duct exit before and after assembly of the diffuser. Static pressure holes were 1mm in diameter and the readings were taken through an inclined alcohol manometer.

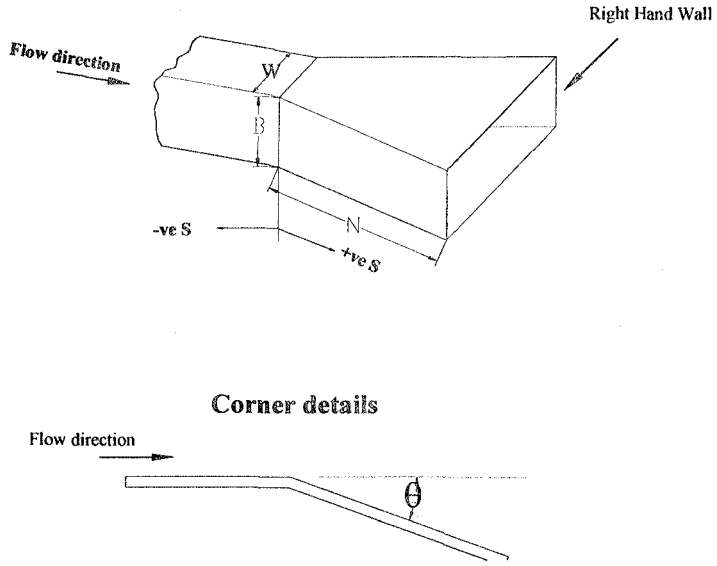

S=100mm N=640mm B=200mm $\theta=25^0$ Boundary layer blockage factor, $2\delta^*/W=0.04$

Figure 1. Diffuser configuration and geometry

The pressure recovery data was taken with reference to the static pressure measured at S/W of –9.24. This position was chosen from evidence of preliminary tests, which showed that once the diffuser was installed, the boundary layer development for the two opposite walls was unsymmetrical as the diffuser inlet was approached. The presence of the diffuser severely distorted the velocity distribution at the inlet duct exit. The velocity distribution for this location was confirmed to be symmetrical and hence the wall static pressure was assumed to be equal to the static pressure on that plane

The inlet conditions were established for all Reynolds number tested. The boundary layer blockage factor was established by use of Eq.1 (Norbury 1959) and although it slightly varied for the different Reynolds number, the value of $2\delta^*/W$ known as the boundary layer blockage factor was practically constant at 0.04.

$$\frac{2\delta^*}{W}=\frac{1}{W}\int_0^W\left(1-\frac{u}{u_c}\right)dy \quad \text{..... 1}$$

where u is the velocity at any position and u_c is the centerline velocity.

The velocity measurements were carried by use of a carefully flattered total pressure tube of 1mm in diameter. The traverse locations were achieved by use of a potential meter scale. Near the wall, the velocities were measured in fine steps of 0.2mm. The Reynolds number was based on centerline velocity and the inlet duct geometry.

The coefficient of pressure recovery thus as presented in this paper was obtained according to Eq.2 (Waitman *et al.* 1961):

$$C_{pr} = \frac{P_{ws} - P_1}{\frac{1}{2}\rho_{air}u_{1c}^2} \qquad \ldots\ldots\ldots\ldots\ldots\ldots \quad 2$$

where P_{ws} is the wall static pressure measured along the diffuser side wall

P_1 is the wall static pressure measured at diffuser inlet taken as S/W = -9.24

u_{1c} is the centerline velocity at the diffuser inlet

In case the reference pressure used was the atmospheric pressure, the term static pressure coefficient C_p (Waitman *et al.,* 1961) is used. Thus

$$C_p = \frac{P_{ws} - P_{atm}}{\frac{1}{2}\rho_{air}u_{1c}^2} \qquad \ldots\ldots\ldots\ldots\ldots\ldots \quad 3$$

To be able to establish the average flow structure, it was necessary to utilize the flow visualization methods. The first method used was the oil flow method. This was done with the oil spread on the diffuser floor and also on a plate, which was introduced at the middle plane running parallel to the roof and the floor. The plate was necessary in order to give an indication of any variation of the flow structure during the subsequent tuft flow visualization method. The plate was secured firmly from underneath by use of thin tape.

The oil was a mixture of red oxide powder, turpentine and liquid paraffin in appropriate ratios. The streamlines thus formed when the flow was introduced were printed on an absorbent paper for later reference and also photographed through a digital camera for all the conditions tested. At low velocities, the oil mixture could not spread well while at very high velocities, the oil spread rapidly and did not give any indication of the streamlines. Flow visualization experiments were therefore carried out for Reynolds numbers of 1.62×10^5 and 2.45×10^5.

After these experiments, the plate was then prepared for the tuft technique. 0.7mm holes to secure firmly 50mm long needles were drilled. The needles were put in a 20mm horizontally and 25mm axially mesh. 20mm long wool tufts were tied to the ends of these needles. They were put in boiling water for sometime to rid them of any oil and to relax their texture before they were finally fixed to the tuft plate. Since the tufts were

white in colour, the plate was painted black to ensure a good contrast in the photographs. The sides of the diffuser were blocked from any reflections by use of black papers.

To be able to establish the flow structure for at different positions from the floor of the diffuser, thin rods of diameter 1mm were prepared to secure the tuft plate at the same horizontal plane throughout its axial length. Since they were underneath the plate, it was not expected that they would have any influence on the flow structure above it. Strictly speaking, the introduction of the tuft plate provided two diffusers of different aspect ratios. The rods were 25, 50, and 125mm in length.

The photographs were taken by use of a digital camera. The camera was fixed along the axial centerline at 205mm from the geometric inlet of the diffuser and at a height of 115mm. The camera was secured on a movable frame and its position could thus be easily varied. All the experiments were carried out at night when there was sufficient darkness. The lighting was provided through a laser beam.

3.0 RESULTS AND DISCUSSION

To establish the inlet conditions for the study, the velocity distribution for the four Reynolds number were measured as shown in Figure 2. The boundary layer thickness was almost the same for all the conditions. However, data for flows very near the wall for Reynolds number 7.2 x 10^4 were slightly different. This could be attributed to the low velocities here and the response time, which was very long due to the small size of the total pressure probe.

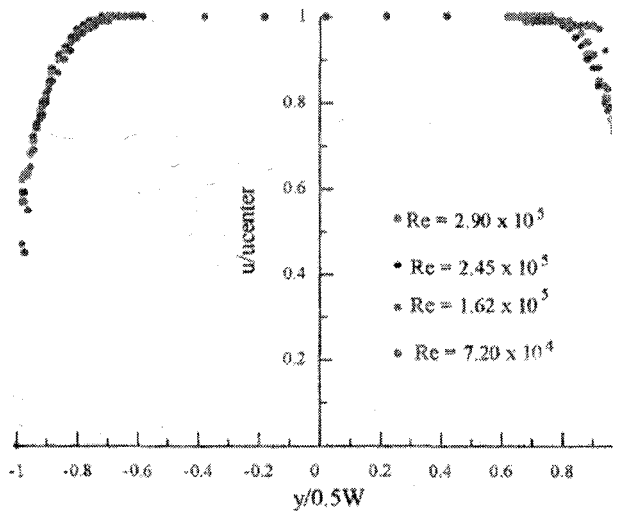

Figure 2. Velocity distribution at S/W=-9.24

Figure 3 shows the coefficient of pressure recovery for Reynolds number of 2.45 x 10^5. The measurements were carried out for both right hand stall and left hand stall. The stalled side could easily be switched from one wall to the other by simply temporarily blocking the unstalled wall side at the exit. Measurements were taken for both the stalled and the unstalled walls. There was no effect in terms of pressure recovery when the walls were switched and the flow could be reproduced. This is in agreement with earlier works of Kline (1959) and Smith and Kline (1974). Consequently all the other experiments were based on right wall stall. Flows for Reynolds number 7.2 x 10^4, 1.62 x $10^5$and 2.9 x 10^5 portrayed similar results.

As found out by Ashjaee and Johnston (1980) and Waitman *et al.* (1961), the influence of Reynolds number on the coefficient of pressure recovery though present does not seem to be significant as can be seen from Figures 4 and 5. Upstream of the diffuser, the static pressure distribution is not influenced by the Reynolds number.

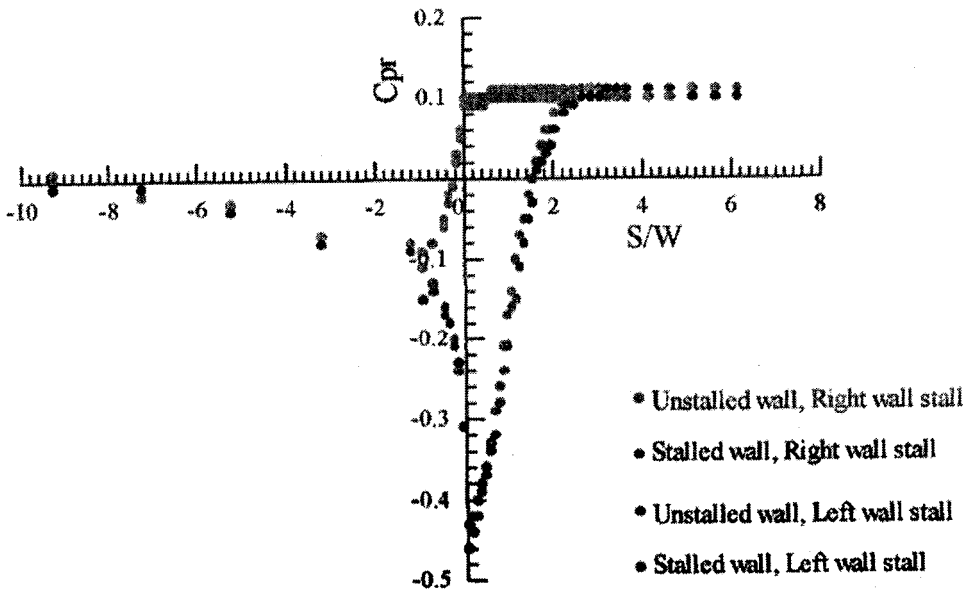

Figure 3. Coefficient of pressure recovery for Re=2.45 x 10^5 and $2\theta=50^0$

However, as the Reynolds number is raised, it is expected that the exit blockage factor would decrease (Wolf and Johnston 1969; Johnston and Powers 1969). This is followed by an increase in the static pressure. The flow near the inlet was characterized

by severe instability and a small recirculating region at the entry was thought to exist. The flow visualization methods show that the end of this point is coincident with the first point of maximum pressure recovery of the unstalled wall. A theoretical explanation of this coincidence requires some further investigation.

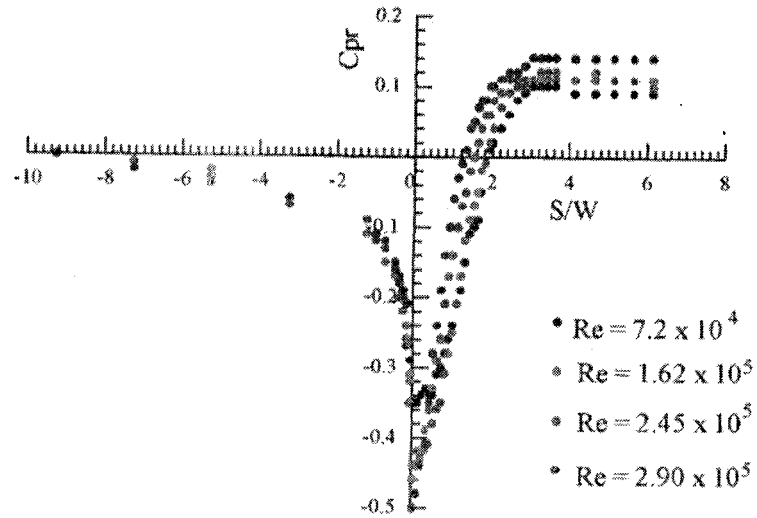

Figure 4. Reynolds number dependence test for the unstalled wall based on Right wall stall for $2\theta=50^0$

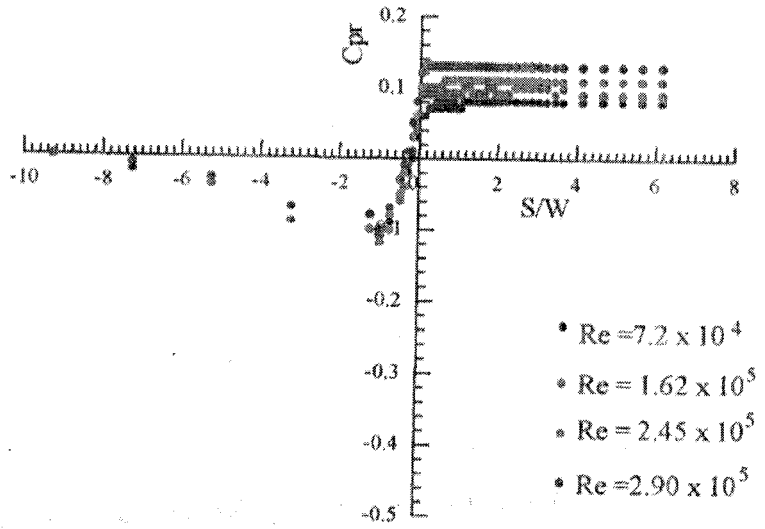

Figure 5. Reynolds number dependence test for the stalled wall based on Right wall stall for $2\theta=50^0$

Figure 6 shows the data repeatability test. Though this flow was highly unstable, the pressure recovery data could be reproduced very accurately.

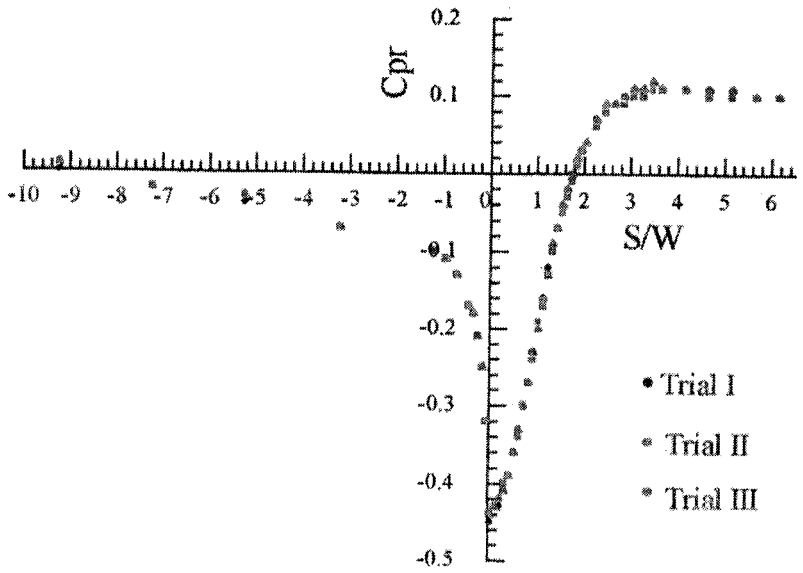

Figure 6. Data repeatability test for unstalled for Re= 2.45 x 10^5 and $2\theta=50^0$

This phenomenon agrees well with the findings of Smith and Layne (1979). It is however expected that the flow structure would be very much time dependent. The pressure recovery data could not tell the time dependence characteristics of the flow. The instability could be seen from the violent swirling of the tufts. A detailed static pressure investigation on the parallel walls of the diffuser is obviously desired from the indications of these findings.

To be able to see the influence of the tuft plate on the macroscopic nature of the flow, measurements of static pressure distributions were carried out. This is shown in Figure 7. As expected, there was a pressure build up within the inlet duct and the diffuser entry region. Again from the point where the entry recirculating region ended, the coefficient of static pressure recovery is unaffected by the introduction of the plate. It was therefore expected that qualitatively the flow structure within the diffuser in the absence of the plate would be similar.

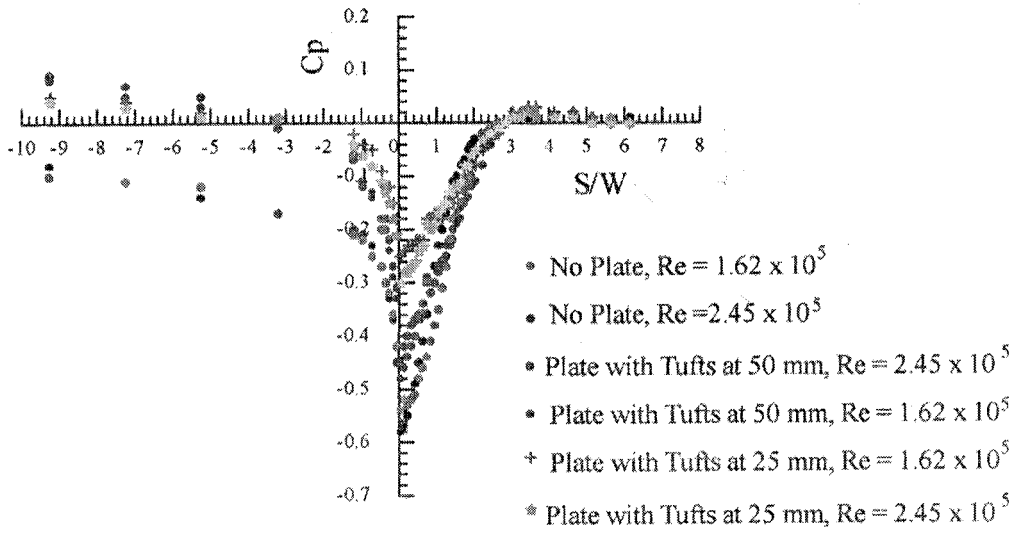

Figure 7. Influence of the tuft plate on static pressure distribution

Figure 8 shows the typical streamline profile obtained by use of the oil flow method. There are four distinguishable regions from the photograph. The first one is the entry-recirculating region. The oil in this region remained almost stagnant with weak motion tendency towards the entry. It was a thin region whose apex was at the diffuser inlet. The streamlines from the stalled wall seemed to deflect and merge at the point where the entry-recirculating region ended. Earlier work performed on rounded diffuser inlet does not report existence of this section. On the stalled side the streamlines curved towards the unstalled wall before getting to the entry region. This was an indication that separation for this wide-angle diffuser may have occurred within the inlet duct consistent with the findings of Feil (1964).

The second one is the stalled region. In this region, the oil did not form any streamlines. This indicated either very weak flow or no flow at all. The tuft method as shown in Figure 9 confirmed this motion to be in the reverse direction and very weak. This reverse motion got stronger as Reynolds number was increased.

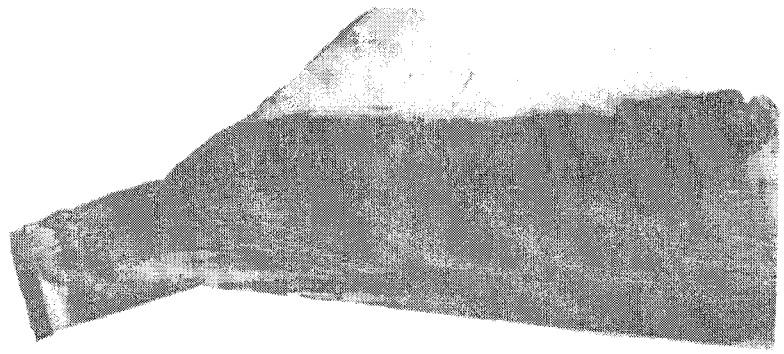

Figure 8. Right hand stall for Re=1.62 x 10^5 and 2θ=50^0 with the plate at 100mm from the bottom plate

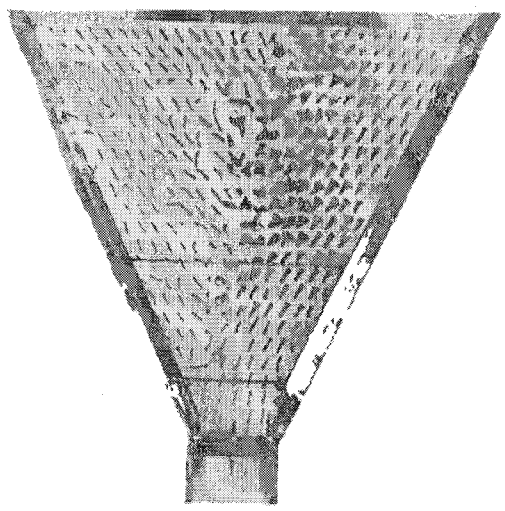

Figure 9. Right hand stall Re=2.45 x 10^5 for 2θ=50^0 Tufts are at 100mm from diffuser floor

The third region is near the exit. This appears near the boundary of the stalled region. The streamlines here indicated existence of a vortex. The tufts in this region were very vibrant and unstable and could change direction very randomly. This region could not easily be detected from the static pressure distribution profiles and further work on detailed static pressure distribution on both the roof and the floor is recommended.

The fourth region was formed near the wall where the streamlines almost ran parallel to the diverging wall. Both the tuft and oil flow methods clearly show this region. The tufts in this region were quite stable and always faced downwards. Figure 10 shows the details of the entry-recirculating region. It can be seen that the tufts near the wall from a length of 175mm from the inlet are facing backwards while slightly further away from the wall the tufts are facing forward. This is the point marked F in Figure 11 and it remained fixed for all the Reynolds number. It was however shifting when the position

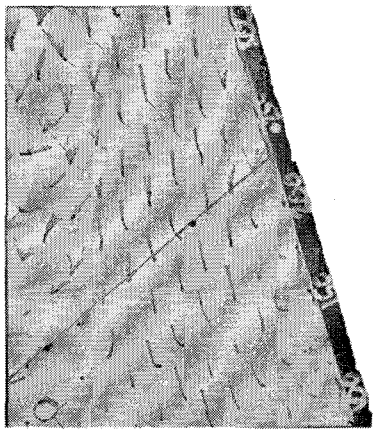

Figure 10. Right hand stall Re= 2.45 x 10^5 and $2\theta=50^0$ Tufts are at 100mm from the diffuser floor: Details of entry-recirculating region

of the tuft plate was altered.

Figure 11 gives the summary of the regions as obtained to scale from the photographs. The following deductions could be made from all the photographs obtained:

Four regions exist.

Region A: Completely stalled region of reversed flow. Tufts were always facing backwards and the flow was calm. The flow here was weak at low Reynolds number. The size of this region seemed to reduce as the plate was lowered indicating that the flow structure would be totally different in the absence of the plate.

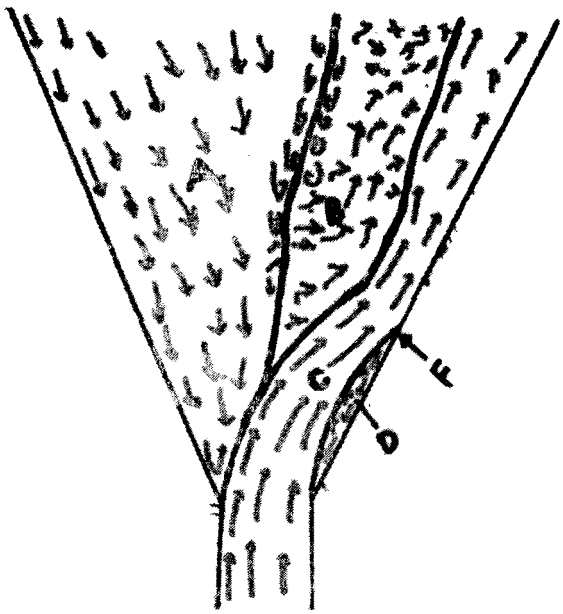

Figure 11. The four regions within the diffuser

Region B: Highly unstable region. Most of the time the tufts were facing downwards but occasionally swirled very fast to face upwards. They vibrated quite rigorously and the intensity went up as Reynolds number was increased. The size of the region increased as the plate was moved down.

Region C: Forward flow region. Tufts assumed almost a fixed direction and although the direction were slightly inclined towards the wall generally they ran almost parallel to the diverging wall. This region became narrower as the plate was lowered.

Region D: Entry recirculating region. The tufts near the wall were always facing upwards and were fairly stable.

The flow visualization study also revealed that:

i) In terms of flow structure, it did not matter which wall was stalled.

ii) The flow structure seemed to be independent of Reynolds number apart from the tuft instabilities of region B.

iii) The point marked F in Fig.11 which was the last tuft near the wall from the entry to face backwards remained fixed at 175mm from the entry even as Reynolds number was varied.

4.0 CONCLUSIONS

The following conclusions may be drawn from this study:

(i) The coefficient of pressure recovery was not strongly affected by Reynolds number

(ii) The presence of the diffuser severely affected the pressure distribution upstream in the inlet duct.

(iii) The pressure recovery data was reproducible, though the flow was highly unstable

(iv) Introduction of the tuft plate did not strongly affect the coefficient of pressure recovery downstream of the entry-recirculating region.

(v) From the flow visualization studies, four regions were seen to exist

A: Completely stalled region

B: Highly unstable region

C: Forward flow region

D: Entry recirculating region

(vi) These regions were not affected by the change in Reynolds number.

The revelation of the four flow regions in this paper, which shows the flow pattern in the entire flow field within the diffuser, eases the burden of getting the correct boundary conditions during numerical modelling for stalled diffuser flows. Future work will investigate the relationship between the geometry of these regions with the diffuser geometry in terms of length to width ratios, aspect ratios at diffuser entry and the total included angle. The effect on the regions due to introduction of a tail-end duct will also be investigated.

REFERENCES

Ashjaee J. and Johnston J.P. (1980). Straight-Walled Two-Dimensional Diffusers-Transitory Stall and Peak Pressure Recovery. *ASME, J. Fluid Eng.*,**102,** 275-282.

Carlson J.J., Johnston J.P. and Sagi C.J. (1967). Effects of Wall Shape on Flow Regimes and Performance in Straight, Two-Dimensional Diffusers, *ASME, J. Basic Eng.*, **189,** 151-160.

Feil O.G. (1964). Vane Systems for Very-Wide-Angle Subsonic Diffusers, *ASME, J. Basic Eng.*, **86,** 759-764.

Johnston J.P. and Powers C.A. (1969). Some Effects of Inlet Blockage and Aspect Ratio

on Diffuser Performance, *ASME, J. Basic Eng.*, **91,** 551-553.

Katelnbach H.J., Fatica M. and Mittal R. (1999). Study of Flow in a Planar Asymmetric Diffusers Using LES, *J. Fluid Mech.*, **121,** 151-185.

Kline S.J. (1959). On the Nature of Stall, *ASME, J. Basic Eng.*, **81,** 305-320.

Norbury J.F. (1959). Some Measurements of Boundary Layer Growth in a Two-Dimensional Diffuser, *ASME, J. Basic Eng.*, **81,** 285-296.

Reneau L.R., Johnston J.P and Kline S.J. (1967). Performance and Design of Straight Two-Dimensional Diffusers, *ASME, J. Basic Eng.*, **89,** 141-150.

Schlichting H. (1955). Boundary Layer Theory, McGraw-Hill Book Company, 7th edition

Senoo Y. and Nishi M. (1977). Prediction of Flow Separation in a Diffuser by a Boundary Layer Calculation, *ASME, J. Fluid Eng.*, **99,** 379-389.

Smith C.R. Jr. and Kline S.J. (1974). An experimental investigation of the transitory stall regime in two dimensional diffusers, *ASME, J. Fluid Eng.* **96,** 11-15.

Smith C.R. and Layne J.L. (1979). An Experimental Investigation of Flow Unsteadiness Generated by Transitory Stall in Plane Wall Diffusers, *ASME, J. Fluids Eng.*, **101,** 181-185.

Waitman B.A., Reneau L.R. and Kline S.J. (1961). Effects of Inlet Conditions on Performance of Two-Dimensional Subsonic Diffusers, *ASME, J. Basic Eng.*, **83,** 349-360.

Wolf S. and Johnston J.P. (1969). Effects of Non-Uniform Velocity Profiles on Flow Regimes and Performance in Two-Dimensional Diffusers, *ASME, J. Basic Eng.*, **91,** 462-474.

Woolley L.R. and Kline S.J. (1978). A Procedure for Computation of Fully Flows in Two-Dimensional Passages, *ASME, J. Fluids Eng.*, **100,** 181-186.